01 Feb 2005

Improving Voltage Stability by Reactive Power Reserve Management

Feng Dong

Badrul H. Chowdhury
Missouri University of Science and Technology, bchow@mst.edu

Mariesa Crow
Missouri University of Science and Technology, crow@mst.edu

Levent Acar
Missouri University of Science and Technology, acar@mst.edu

Recommended Citation

F. Dong et al., "Improving Voltage Stability by Reactive Power Reserve Management," *IEEE Transactions on Power Systems*, vol. 20, no. 1, pp. 338-345, Institute of Electrical and Electronics Engineers (IEEE), Feb 2005.
The definitive version is available at https://doi.org/10.1109/TPWRS.2004.841241

Improving Voltage Stability by Reactive Power Reserve Management

Feng Dong, *Student Member, IEEE*, Badrul H. Chowdhury, *Senior Member, IEEE*, Mariesa L. Crow, *Senior Member, IEEE*, and Levent Acar, *Senior Member, IEEE*

***Abstract*—The amount of reactive reserves at generating stations is a measure of the degree of voltage stability. With this perspective, an optimized reactive reserve management scheme based on the optimal power flow is proposed. Detailed models of generator limiters, such as those for armature and field current limiting must be considered in order to utilize the maximum reactive power capability of generators, so as to meet reactive power demands during voltage emergencies. Participation factors for each generator in the management scheme are predetermined based on the voltage-var (V-Q) curve methodology. The Bender's decomposition methodology is applied to the reactive reserve management problem. The resulting effective reserves and the impact on voltage stability are studied on a reduced Western Electric Coordinating Council system. Results prove that the proposed method can improve both static and dynamic voltage stability.**

***Index Terms*—Bender's decomposition methodology, optimal power flow, reactive power management, voltage collapse.**

I. Introduction

VOLTAGE collapse typically occurs on power systems which are heavily stressed. It may or may not be initiated by a disruption, but is usually characterized by shortage of fast-acting reactive reserves. Voltage collapse often involves specific areas of the power system, although the entire system may also be involved. Many system variables may participate in this phenomenon. However, some physical insight into the nature of voltage collapse may be gained by examining the production, transmission and consumption of reactive power. Voltage collapse is associated with reactive power demands not being met because of limitations on the production and transmission of reactive power [1]. Reactive power demand generally increases with a load increase, motors stalling, or a change in load composition such as an increased proportion of compressor load. The fast reactive sources are generators, synchronous condensers and power electronics-based flexible ac transmission systems (FACTS). During voltage emergencies, reactive resources should activate to boost transmission voltage levels. This action reduces reactive losses of transmission lines and transformers, and increases line charging and shunt capacitor outputs. In the mid-term time scale, a voltage collapse usually does not happen until most of the large reactive power resources reach their respective reactive power limits. Generally, one or two critical resources reaching their limits can spawn cascading limiting effects at neighboring units. Hence it is wise to keep enough reserves in order to improve the voltage stability margin.

Reactive power margins have always been linked with voltage stability. The Western Electric Coordinating Council (WECC) specifies the voltage stability criteria in terms of real and reactive power margins [1]. The minimum reactive power margin is determined by the voltage-var (V-Q) curve method. The V-Q method has been well studied [1]–[3]. Reference [4] discusses a reactive management program for a practical power system. The authors discuss a planning goal of supplying system reactive demands by installation of properly sized and properly located capacitor banks which will allow generating units to operate at or near unity power factor. However, it is a cost-intensive proposition. Besides, this strategy is not always very effective since not all the shunt capacitors are fully utilized. Reference [5] uses the reactive power margins to evaluate voltage instability problems for coherent bus groups. These margins are based on the reactive reserves of generators and static var compensators (SVCs) that exhaust reserves in the process of computing a V-Q curve at any bus in a coherent group or voltage control area. The authors in [6] discuss a hierarchical optimization scheme which optimizes a set of corrective controls such that the solution satisfies a given voltage stability margin. Bender's decomposition is employed to handle stressed cases. In [7], the authors introduce a methodology to reschedule the reactive injection from generators and synchronous condensers with the aim of improving the voltage stability margin. Their method is formulated based on modal participations factors and an optimal power flow (OPF) wherein the voltage stability margin, as computed from eigenvectors of a reduced Jacobian, is maximized by reactive rescheduling. However, the authors avoid using a security-constrained OPF formulation and thus the computed voltage stability margin from the Jacobian would not truly represent the situation under a stressed condition.

In [8], the authors employ a security-constrained OPF for optimal var expansion planning design. The OPF is solved twice—once with simply the voltage profile constraint and then with a pre-selected voltage stability margin criterion. The larger of the two solution is then selected for the combined solution.

In this paper, a reactive reserve management program (RRMP) based on an optimal power flow is proposed to manage critical reactive power reserves. A multi-objective function specifically for this purpose is introduced. This

Manuscript received May 26, 2004. Paper no. TPWRS-00134-2004.

The authors are with the Electrical and Computer Engineering Department, University of Missouri-Rolla, Rolla, MO 65409 USA (e-mail: bchow@ece.umr.edu).

Digital Object Identifier 10.1109/TPWRS.2004.841241

function is used in a mixed-integer nonlinear optimization formulation. Various generators are assigned different weights in order to maintain maximum reactive reserves within the areas that are most vulnerable to voltage instability problem. A decomposition technique is adopted to formulate subproblems with various stress levels. The nonlinear interior point method (NIP) is then used to solve the separate subproblems. The advantage in this formulation is that the system is able to maintain a specified voltage stability margin, and at the same time, raise its level of voltage stability. The proposed method is tested on a reduced WECC system with 283 buses and 29 generators.

II. Optimization Framework

A. Reactive Reserves

The reactive power sources consist of synchronous generators and shunt capacitors and reactors on the transmission network. During a disturbance, the real power component of line loadings does not change significantly, whereas the reactive power flow can change dramatically. The reason is that the voltage drops resulting from the contingency decreases the reactive power generation from line charging and shunt capacitors, thereby increasing reactive power losses. Sufficient reactive reserves should be available to meet the var changes following a disturbance. Simply speaking, the reactive power reserve is the ability of the generators to support bus voltages under increased load condition or system disturbances. How much more reactive power the system can deliver depends on the operating condition and the location of the reserves, as well as the nature of the impending change.

The reserves of reactive sources can be considered a measure of the degree of voltage stability. As a matter of fact, BPA—a transmission provider in the western United States—considers reactive reserves at major generating plants to be a critical indicator of voltage stability and, consequently, the agency has installed a reactive power monitor [9] at critical hydroelectric power stations that serve its service area.

The available reactive power reserve of a generator is determined by its capability curves [10]. It is worth noting that for a given real power output, the reactive power generation is limited by both armature and field heating limits.

The active and reactive power generation output at a synchronous generator may be represented as [10]

$$P_g = \frac{E_q V_g}{X_d}\sin\delta + \frac{V_g^2}{2}\left(\frac{1}{X_d} - \frac{1}{X_q}\right)\sin 2\delta \tag{1}$$

$$Q_g = \frac{E_q V_g}{X_d}\cos\delta - V_g^2\left(\frac{\sin^2\delta}{X_d} + \frac{\cos^2\delta}{X_q}\right) \tag{2}$$

where $\mathrm{V_g}$ is the terminal voltage of the generator based on the per unit system and $E_q = i_{gfd}$, where i_{gfd} is the field current. In order to write an analytical model to relate the reactive power limit to the maximum field current, we use a cylindrical rotor model with $X_d = X_q$. Thus, from (1) and (2), the maximum reactive power with respect to the field current limit may be obtained as

$$Q_{g\max} = -\frac{V_g^2}{X_d} + \sqrt{\frac{V_g^2 I_{gfd\max}^2}{X_d^2} - P_g^2}. \tag{3}$$

Thus, the maximum reactive power $Q_{g\max}$ of the generator is determined by the maximum field current $I_{gfd\max}$. The relationship also shows that the maximum reactive generation is a function of the terminal voltage. The maximum reactive power output should also satisfy the armature current limitation as follows:

$$Q_{g\max} = \sqrt{V_g^2 I_{ga\max}^2 - P_g^2}. \tag{4}$$

The reactive power reserve of the gth generator is then represented as

$$Q_{g\max\mathrm{res}} = Q_{g\max} - Q_g \tag{5}$$

where $Q_{g\max}$ is the smaller of the two values obtained from (3) and (4) and Q_g is the reactive power output under normal operating conditions. A generator's reactive reserve is calculated by (5) if Q_g is lower than $Q_{g\max}$. However, if Q_g reaches its limit, the reactive reserve is set to zero and Q_g varies as a function of the terminal voltage.

B. Mathematical Formulation

The RRMP is formulated as an optimal search problem whose primary objective is to maximize the effective reactive reserves under normal operating conditions to ensure higher voltage stability margin. A secondary objective is to minimize losses subject to various operational constraints. The dual-objective RRMP is therefore formulated as follows.

Objective function

$$F(U) = \mathrm{Min}\{p_1 Q_{\max\mathrm{res}} + p_2 P_{\mathrm{loss}}\} \tag{6}$$

where $Q_{\max\mathrm{res}}$ is the sum of reactive reserves of the system to be optimized, that is, $Q_{\max\mathrm{res}} = \sum w_g Q_{g\max\mathrm{res}}$; $Q_{g\max res}$ is the reactive power reserve of the gth generator; w_g is weight factor of the gth generator and is discussed in the following section, and P_{loss} represents the transmission losses. Since we have a dual objective of maximizing reactive reserves and minimizing transmission losses, we pick $p_1 < 0.$ and $p_2 > 0.$

The constraints to the above optimization are

$$\left.\begin{aligned} P_i &= V_i \textstyle\sum_{j=1}^{n} V_j (G_{ij}\cos\theta_{ij} + B_{ij}\sin\theta_{ij}) \\ Q_i &= V_i \textstyle\sum_{j=1}^{n} V_j (G_{ij}\sin\theta_{ij} - B_{ij}\cos\theta_{ij}) \quad i \in N \end{aligned}\right\} \tag{7}$$

$$\begin{cases} T_{i\min} < T_i < T_{i\max}, & i \in N_T \\ V_{gi\min} < V_{gi} < V_{gi\max}, & i \in N_G \\ Q_{Ci\min} < Q_{Ci} < Q_{Ci\max}, & i \in N_C \end{cases} \tag{8}$$

$$V_{\mathrm{li}\min} < V_{\mathrm{li}} < V_{\mathrm{li}\max} \quad l \in N_L \tag{9}$$

$$Q_{gi\min} < Q_{gi} < Q_{gi\max} \quad i \in N_G \tag{10}$$

where

V_i	voltage magnitude at load bus i;
θ_{ij}	voltage angle difference between bus i and bus j;
G_{ij}, B_{ij}	elements ij of the admittance matrices;
P_i, Q_i	active/reactive power injected into network at bus i;
N_T, N_G, N_C, N_L	total number of transformers, generators, shunt capacitive/reactive installations, and loads, respectively;
U	control variables;
$T_{i\max}/T_{i\min}$	limits of tap setting of transformer branch i;
$V_{gi\max}/V_{gi\min}$	limits of voltage at generator bus i;
$Q_{Ci\max}/Q_{Ci\min}$	compensation capacity limits at bus i;
$V_{\mathrm{li}\max}, V_{\mathrm{li}\min}$	limits of voltage at load bus i;
$Q_{gi\max}/Q_{gi\min}$	reactive power capacity limits at gen bus i.

The voltage stability constraints may be written as

$$Q_k^C \geq Q^N + \beta S_t S^{\mathrm{margin}} \tag{11}$$

where Q_k^C is the reactive load for the kth stressed case in the set "C", $k = 1, \ldots, M$, and M is the total number of stressed cases; Q^N is the reactive load under normal condition; $\beta = [\beta_1, \beta_2 \ldots, \beta_{N_L}]'$ is a direction of load increase; S_t is the total reactive load under normal condition; S^{margin} is the specified reactive margin. For example, β_i is the relative increase in the load at bus i with respect to the system load increase, where $\sum_{i \in N_L} \beta_i = 1$.

A power system can be stressed from the current operating point to the collapse point by increasing the reactive loads in several directions. In some directions, the system may have insufficient reactive power margin to guarantee voltage security. These cases are grouped into one set, which will be called "C". These critical cases are determined in the third step during assignment of weight factors of participating generators, as discussed at the end of Section II. By satisfying constraint (11), the system has a minimum reactive margin required for secure operation. Ensuring all voltage control areas to have the minimum reactive margin is equivalent to all stressed cases being feasible under the operation constraints.

The intent in the above formulation is not only to satisfy the voltage stability criteria but also to improve voltage stability. Thus, if (11) is satisfied in the optimization, the system is guaranteed to be voltage stable and optimizing var reserve in (6) would not be needed if stability was not to be improved. Without the aforementioned objective function, it is possible that some strong areas in the system may rob weaker areas of the much-needed reactive reserves.

C. Determination of Area Weights

Under an ideal operating condition, all generators operate at unity power factor so the system possesses the maximum reactive reserve possible. However, it is extremely difficult to implement such an operating condition in real power systems. Secondly, given all generators are equally weighted, maximizing the reactive reserves for the entire system is both inefficient and inadequate. Attempting to maximize reactive reserves at generators as an operational optimization measure with equal participation throughout a system may lead to undesirable consequences such as depleting reserves at generators which are critical to maintaining voltage stability in the event of a disturbance.

It is well known that the voltage instability phenomenon is essentially a local problem, wherein some weak areas become prone to voltage collapse because of shortage of reactive power. These areas need higher reactive power reserves than others when subjected to the same voltage emergency. In [5], the author discusses the importance of dividing the power network into voltage control areas because each area exhibits vulnerability to a disturbance in a different way. With the same objective in mind, we have separated the entire network into voltage control areas with the basic idea being that the weakest transmission element connected to each bus is identified by a scalar parameter α. The parameter α is determined such that the V-Q curve minima in computing the V-Q curve minimum at a bus are almost identical for all buses in one voltage control area. The groups of buses that remain interconnected, after the weak transmission elements are eliminated, define the voltage control areas. The reactive power-voltage relationship given by the Jacobian matrix element J_{QV} is used to measure electrical distance between any two nodes. The off diagonal Jacobian matrix elements with the smallest absolute values indicate the weak connections or long electrical distances between corresponding buses and are therefore eliminated from each row until the sum of the elements eliminated is less than or equal to αd, where $d = \max\{J_{\mathrm{QV}}\}_{ii}$. The buses corresponding to the remaining elements in the Jacobian are grouped into one voltage control area. Then, the V-Q curve at any bus within each control area is computed to find the reactive margin of this area.

The bottom of the V-Q curve is the maximum reactive load that a system can sustain. The distance from this point to the operating point is usually considered the reactive power margin at the bus [3]. Using this method, we can reliably claim that the area that has the smallest reactive margin is the most vulnerable to voltage instability. At the minima of the V-Q curve, the reactive reserves of generators that are depleted are the effective reserves for this area and, thereby, determine the reactive margin in the area. The amount of effective reserves is a key index in voltage stability assessment. Therefore, an objective of the proposed RRMP is to maximize the effective reactive reserves in the system. These reserves associated with each voltage control area are assigned a weight according to

$$w_g = \frac{S_t S^{\mathrm{margin}}}{Q_i^{\mathrm{margin}}} \tag{12}$$

where Q_i^{margin} is the reactive margin of the area.

To summarize, the procedure for weight factors is as follows.

1) Divide the network into voltage control areas as specified above.

2) Determine the reactive margin for each area by the V-Q method.
3) Determine the weights for each generator based on the specific margins in each area.

III. Stressed Case Subproblem

By considering the reactive margin constraints of (11), the constrained optimization problem (6)–(11) becomes one of reactive reserve management with dynamic security constraints. At the optimal point, the system has the maximum reactive reserves under normal operation condition, and each case in set C is feasible. It can be hierarchically decomposed into two parts, a base case subproblem and a stressed case subproblem that can be solved by the Bender's cuts decomposition method [11]–[13]. For some stressed cases, the power flow may become infeasible. However, in order to apply a decomposition methodology, there is a need to have some measure of this infeasibility. Since this kind of infeasibility is caused by reactive power load increase, fictitious reactive injections are used as slack variables and added to the constraints corresponding to the reactive power balance equation at a bus. Therefore, the objective function for the stressed cases is to minimize the sum of the fictitious injections of reactive power. If the fictitious injections are equal to zero, then we claim that the stressed case is feasible. The stressed case subproblem may then be stated as shown in the equation at the bottom of the page, where s_{ci} and s_{ri} are fictitious capacitive and inductive power injection, respectively, at bus i. Although, theoretically, fictitious reactive power can be injected at any bus, since the set "C" of critical load directions is given, we select only those buses in this critical set for a load increase. In the above formulation, U is the vector of control variables and U^* is determined by the base case problem.

IV. Algorithm Implementation

The procedure for the two level Bender's decomposition is presented in Fig. 1. The base case subproblem (master problem) is the optimization problem given by (6). Thus, the master problem is formulated as follows:

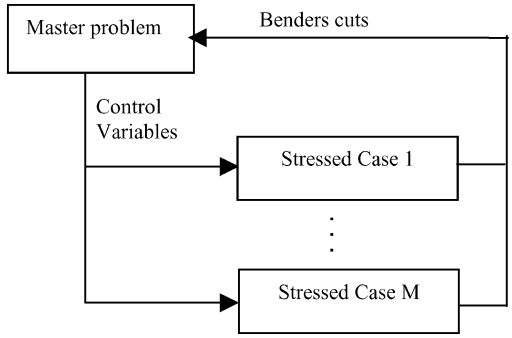

Fig. 1. Two-level hierarchical structure for optimization.

$$\text{Min} \quad F(U) \tag{19}$$

$$\text{Subject to}:$$

$$f(V,\theta,U)=0 \tag{20}$$

$$g(V,\theta,U)\geq 0 \tag{21}$$

$$\text{Bender}'\text{s cuts}:$$

$$S_k(U)\leq 0; \quad k=1,\ldots,M. \tag{22}$$

Each subproblem (13)–(18) (shown at the bottom of the page) at the second level minimizes the fictitious reactive injections for the given values of U^* and returns to the master problem, information about the optimal objective function and its sensitivities with respect to U^*—called Bender's cuts. The procedure is briefly discussed below.

An initial guess of control variables U is obtained by solving the master problem (19)–(22) with $S_k(U)=0, k=1,\ldots,M$. With the given U, the stressed cases are sequentially formulated and solved, and the optimal result of each stressed case is used to update the Bender's cuts. For example, for the kth stressed case subproblem, the value of the objective function $S_k(U)=0$ means that the system has sufficient reactive margin required and that the stressed case is feasible. Alternately, $S_k(U)>0$ means that the stressed case is infeasible with the current control variables. Thus, the more accurate Bender's cuts $S_k(U)=$

$$S_k(U)=\text{Min}\sum_i (s_{ci}+s_{ri}) \tag{13}$$

$$\text{Subject to}:$$

$$\left.\begin{aligned} &P_i = V_i\textstyle\sum_{j=1}^{n} V_j(G_{ij}\cos\theta_{ij}+B_{ij}\sin\theta_{ij}) \\ &Q_i^C - s_{ci}+s_{ri} = V_i\textstyle\sum_{j=1}^{n} V_j(G_{ij}\sin\theta_{ij}-B_{ij}\cos\theta_{ij}) \quad i\in N \end{aligned}\right\} \tag{14}$$

$$U=U^* \tag{15}$$

$$V_{\text{li}\min}<V_{\text{li}}<V_{\text{li}\max} \quad l\in N_L \tag{16}$$

$$Q_{gi\max}<Q_{gi}<Q_{gi\max} \quad i\in N_G \tag{17}$$

$$s_{ci}\geq 0, \quad s_{ri}\geq 0 \tag{18}$$

$S_k(U^*) + \lambda_k(U - U^*)$ in the master problem based on the optimal results are built, where λ_k are the Lagrange multipliers associated with the kth stressed case. The Bender's cuts return to the master problem, the information to remediate infeasibility of the stressed case. The two-stage process is repeated until a U^* is found for which all $S_k(U) = 0, k = 1, \ldots M$. That is, the fictitious injections of reactive power are equal to zero in all stressed case subproblems.

Each subproblem is solved through a NIP. The foundation for interior point methods consist of three building blocks: barrier method for optimization with inequality constraints, Lagrange's method for optimization with equality constraints, and Newton's method for solving nonlinear equations. The master problem is taken as an example to show the application of the NIP. By using slack variables, the problem (19)–(22) is rewritten as

$$\text{Min} \quad F(U) \tag{23}$$

$$\text{Subject to :}$$

$$f(X,U) = 0 \tag{24}$$

$$g(X,U) - s_1 = 0 \tag{25}$$

$$S_k(U) + s_{2k} = 0; \quad k = 1, \ldots, M \tag{26}$$

$$s_1 \geq 0; \quad s_{2k} \geq 0 \tag{27}$$

where X is the vector of state variables, and s_1, s_{2k} are the primary nonnegative slack variables used to transform the inequality constraints to equalities. The inequality constraints are incorporated into the objective function as a logarithmic barrier function. So, barrier functions $\mu_1 \ln s_1$ and $\mu_{2k} \ln s_{2k}$ are introduced with respect to (27). The Lagrange function for the problem (23)–(27) is defined as

$$L = F(U) - \sum \lambda_1^T f(X,U) - \sum \lambda_2^T g(X,U) - \sum \lambda_{3k}^T S_k(X,U) - \mu_1 \ln s_1 - \mu_{2k} \ln s_{2k} \tag{28}$$

where λ_1, λ_2, and λ_{3k} are the Lagrange multipliers, and μ_1 and μ_{2k} are the barrier parameter. At the optimal point, barrier parameters μ_1 and μ_{2k} reach zero. The set of nonlinear equations are derived following optimality conditions and solved by Newton's methods. For the interested reader, [14] and [15] present the interior point method in more detail.

The maximum reactive power generation is calculated to determine whether the limit is reached in each iteration during the subproblem optimal search. If the limit is exceeded, the corresponding generator node is changed to a PQ node, where the reactive power generation becomes a function of the terminal voltage as given by (3)–(4). The generator's reactive reserve is made equal to zero.

V. Case Study

A. Reduced WECC System

A reduced WECC system, geographically representing the western United States, is used to test the RRMP. This system, shown in the Appendix, consists of 283 buses. The entire system is divided into several subareas administratively. These are BC, WA, MT, ID, WY, UT, OR, CO, NM, NV, AZ, and CA. The heavy load area is located in the CA region. Some subareas such as WA, MT etc. are responsible for supplying power to CA via long-distance high-voltage lines. Under normal conditions, there are no operating constraint violations. However, a preliminary analysis shows that there are several weak areas prone to voltage instability. The system is divided into several different voltage control areas using the method discussed in Section II-C. A bus in each area is selected for conducting the V-Q analysis. Table I shows the reactive margins in the nine areas before optimization. It is noted that there are two weak areas—areas 8 and 9 with insufficient reactive margin, *vis-à-vis* 350 and 200 MVAr, respectively. Both areas are in the Northern CA area. The required reactive margin is specified as 450 MVAr, which is 5% of the total reactive load Thus, using $S_t S^{\text{margin}} = 450$ MVAr in (12), we determine the weight factors of effective reserves at each generator as shown in Table I.

TABLE I
Reactive Margin in Areas Before and After Optimization

Area	Initial reactive margin (MVAr)	Weighting factor	Reactive margin with RRMP (MVAr)
1	500	0.9000	750
2	1500	0.3000	1650
3	1800	0.2500	1900
4	800	0.5625	1050
5	800	0.5625	1100
6	1100	0.4091	1200
7	2300	0.1957	2780
8	350	1.2857	550
9	200	2.2500	580

Assuming a dual objective of maximizing reactive reserves and minimizing system losses, $\mathrm{p_1}$ and $\mathrm{p_2}$ in (6) are selected as -1 and 0.1, respectively thereby giving ten times more priority to maximizing the reserves than minimizing the losses. The control variables include voltage set points of 12 out of 28 generators, ten ULTCs, and six shunt capacitors. The set "C" includes five stressed cases. The optimal search starts with the master problem before consideration of the stressed cases. The set points are then sent to the subproblems. e.g., one stressed case is that the total reactive loads in northern CA area are increased by 450 MVAr. The increased reactive demands are proportionally distributed among all loads in this area to each reactive load under normal condition. The value of the objective function of this stressed case is 108.3 MVAr, which means that this stressed case is not feasible. With Bender's cuts, the base case is resolved to calculate a set of control variables. After just one iteration between the master problem and the subproblems, the overall procedure converges and the new set points ensure feasibility for all stressed cases.

The specified reactive margin $S_t S^{\text{margin}}$ has a significant effect on the results and computation time. An unreasonably high reactive margin specified may lead to a null solution set for the optimization problem and necessitate additional reactive compensation devices to meet the reactive margin. Thus, the reactive margin for a system must be determined carefully. Usually, the

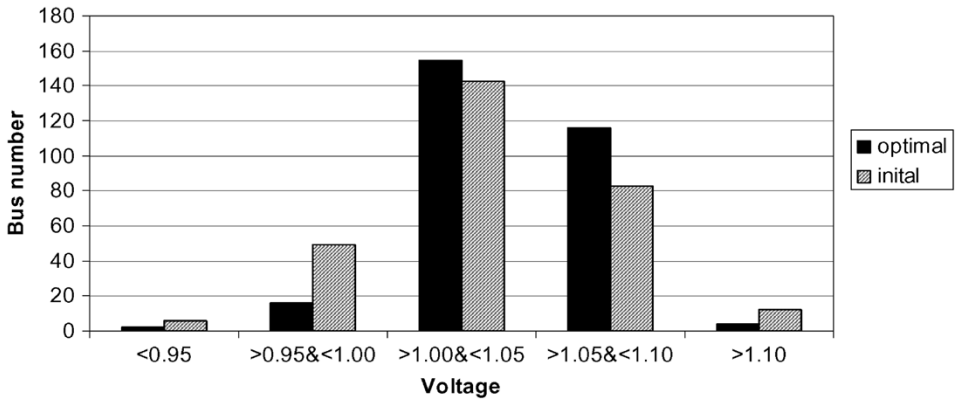

Fig. 2. Voltage profile before and after optimization.

TABLE II
REACTIVE POWER OUTPUT AND VOLTAGE SHCEDULE

GENERATORS	Q_G (MVAR)	V (PU)	Q_G'(MVAR) WITH RRMP	V' (PU) WITH RRMP
CANAD G1-30	1011	1.00	825.05	1.07
BRIDGER2-36	285	1.01	271.87	1.03
INTERM1G-45	534	1.05	443.46	1.01
MONTA G1-65	953	1.00	739.18	1.04
DALLES21-70	431	1.06	-293.33	1.04
JOHN DAY-77	854	1.00	498.42	1.03
NORTH G3-79	1853	1.00	1143.8	1.07
TEVATR-116	192	1.05	76.75	1.00
TEVATR2-118	1653	1.00	1500	1.06

TABLE III
SHUNT CAPACTIOR AND ULTC SHCEDULE

CONTROL VARIABLES	INITIAL	POST-OPTIMIZATION
$ULTC_{113-114}$	0.95 pu	1.02 pu
$ULTC_{48-49}$	1.05 pu	1.01 pu
QC60 (MVAR)	2146	1543
QC80 (MVAR)	1200	866
QC 119 (MVAR)	1500	*1150*

NERC-recommended reactive power criteria for area reliability is a good starting point.

After optimization, the control variables activated include nine generation voltage settings, two shunt capacitors, and two ULTCs. In Tables II and III, voltage, shunt capacitors and tap changer reschedules are listed respectively. In Table II, the fourth and fifth columns are the reactive power outputs and voltages at the generator terminal buses after optimization. Compared with initial conditions, the results show improved reactive power reserves. The voltage profile of the system is also improved as shown in Fig. 2 and the transmission losses are reduced by 45 MW, from 637 MW down to 592 MW.

B. Static Analysis and Dynamic Simulations

In this section, we verify the optimization results from two aspects—static analysis (V-Q curves) and full dynamic simulations. In Fig. 3, two V-Q curves are plotted. Curve "A" is the V-Q curve at bus 112 in area 9 at the initial operating state. From the figure, the reactive margin is 200 MVAr, which is also listed in Table I. After running the RRMP optimization, a V-Q analysis at the same bus reveals that the reactive margin is improved to 500 MVAr, as shown by curve "B". Similar conclusions were drawn by analyzing reactive margins at other voltage control areas.

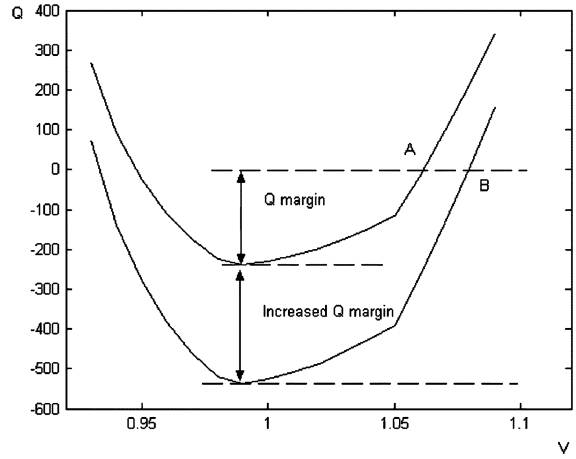

Fig. 3. V-Q curves at bus 112 before and post optimization.

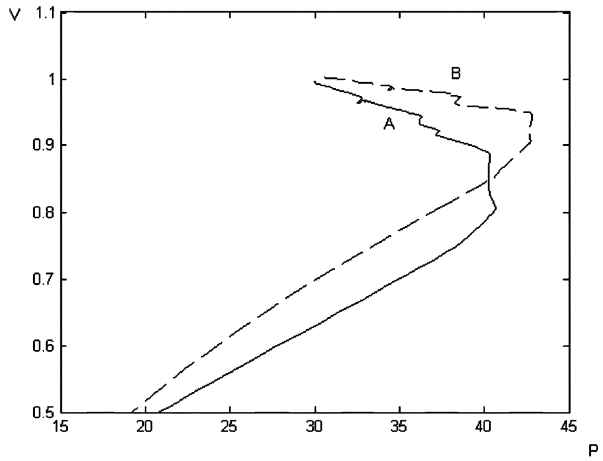

Fig. 4. Real power margin improvement with RRMP.

The improvement in the real power margin after optimization can be seen in Fig. 4. It shows two PV curves. P is the sum of total real power loads and V is the average voltage in area 8. The solid curve A in the figure corresponds to the margin at the initial

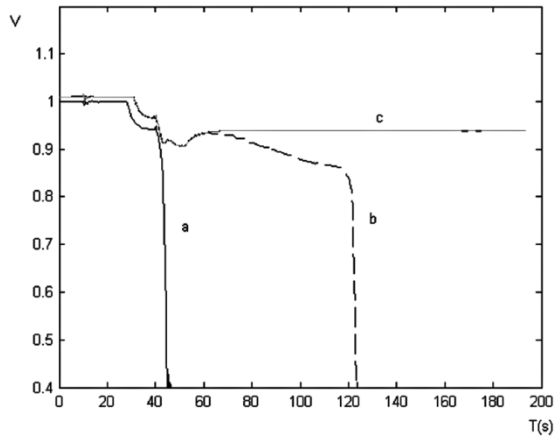

Fig. 5. Voltage trajectory at bus 118.

condition and curve B corresponds to that after optimization. It is obvious that the total real power margin has been extended by 3 p.u. or 300 MW.

We now see how the results of the RRMP impacts dynamic voltage stability. We ran a full time domain simulation of the system subject to the same disturbances both before and after optimization and compared the results. Dynamic models include OELs installed at Gen #118, #148, #138, and #144, 108 ULTCs, as well as ten induction motors in addition to the usual models associated with synchronous generators (exciters, turbine-governors and PSS). In order to reduce simulation computation time, the OEL time constants were deliberately reduced.

The disturbance consists of a sequence of an outage of Gen #112 at 10 s, and outages of both circuits of the line 76–82 at 10 and 40 s, respectively. The software used for the dynamic simulations was EUROSTAG [16].

In Fig. 5, the voltage trajectories at bus 118 are shown with respect to the two cases. Curve "b" is with the optimal operating conditions and curve "a" is with the initial operating conditions. The case with the initial conditions results in a faster voltage collapse when subjected to the above mentioned disturbance. The reasons for the earlier collapse may be summarized as follows: After the trip-off of the first circuit of the line 76–82 and the generator 112, the OEL at generator 118 is enforced at 30 s. Hence, this generator loses voltage control. A large induction motor load IND_119, connected to bus 1119—in close proximity to generator 118, stalls. Then reactive power demand increases rapidly, which eventually sets the collapse in motion. In the other case, the OEL at the same generator 118 delays activation until 35 s due to a higher system voltage profile. The system is strong enough to survive from transient voltage instability as well as the ensuing outage of the second circuit of the line 76–82. After a time delay, ULTCs start to operate to restore voltages on the load side and the system is stressed further. The bus voltages decrease gradually and the reactive power generation from shunt capacitors and transmission lines reduce drastically. Finally the system collapses at 130 s. The longer period until collapse leaves some time for operator intervention so as to initiate some control strategies to prevent the system from collapsing. The proper corrective control in this case would

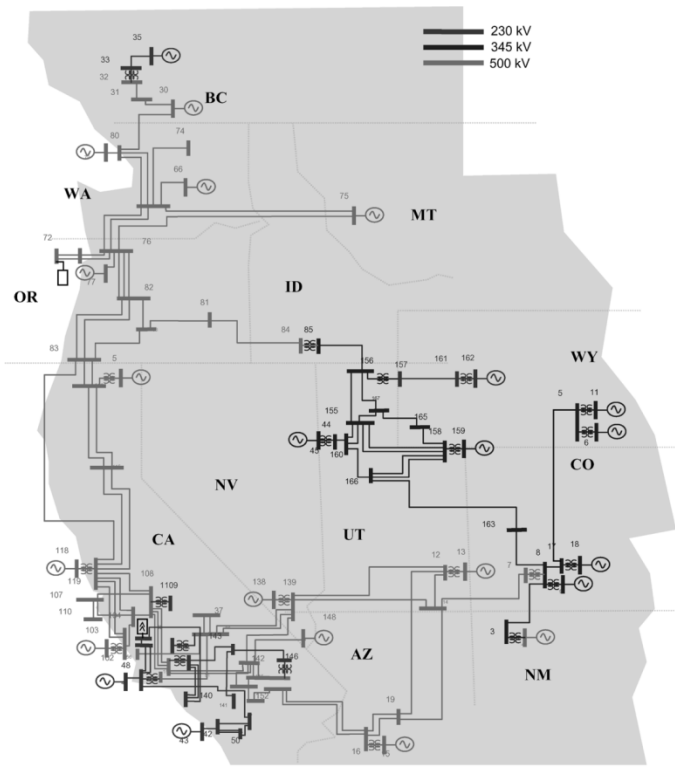

Fig. 6. Reduced WECC System.

have been to block tap changers. By blocking tap changers, the system is voltage stable, shown as curve "c" of Fig. 5. The comparison shows that reactive reserves are beneficial to improve voltage stability.

To compare the above results with a single objective of simply minimizing losses, p_1 and p_2 in (6) were then selected as 0 and 1.0, respectively, thereby ignoring the reactive reserves and minimizing the losses. The constraints were kept the same, and the reactive power margin was still 450 MVAr. In this case, the global optimization problem failed to converge after ten iterations. Two out of five stressed cases were found to be infeasible. The first infeasible stressed case was one where we increased reactive power demand in area 8 by 450 MVAr uniformly distributing the load increase at area buses 113,114, 115, and so on. The second infeasible stressed case was where we increased reactive power demand in area 9 by 450 MVAr, uniformly distributing the load increase at area buses 13, 142, 150, 151, and so on.

At this point, the required reactive margin was decreased from 450 to 300 MVAr and the global optimization problem converged. With the reduced reactive margin, power losses decreased from 637 to 573 MW, which was to be expected. However, three generators (buses 140, 148, and 159) from outside the weak area received additional reactive reserves, while two generators (buses 116 and 118) in the weak area were left unchanged. In addition, two additional ULTCs ($\mathrm{ULTC}_{102\text{–}103}$ and $\mathrm{ULTC}_{161\text{–}162}$) that were outside the weak area were optimized and the output of one new shunt capacitor outside the weak area was reduced. Additionally, the real power margin was reduced to 120 MW.

VI. Conclusion

This paper discusses the management of dynamic reactive power reserves in order to improve voltage stability. The method is based on optimal power flow and the Bender's decomposition technique. The proposed RRMP is decomposed into two parts giving it a hierarchical structure that gives the optimal problem added flexibility. Both armature and field current limiting are introduced into the optimization problem so as to make the model more accurate for mid-term voltage stability analysis. The robust interior point method is utilized to solve the problem. Detailed generator models were considered in the optimization.

Since synchronous generators contain the most effective dynamic reactive reserves, a weighting scheme is designed to select the set of participating generators that have the most influence in strengthening a weak area. The weights were determined by V-Q curves. Both static and dynamic voltage stability margins are improved by managing the reactive reserves at these participating generators. Test studies show that reactive reserves are beneficial for maintaining and improving voltage stability.

The uniqueness in the solution strategy proposed in this paper stems from the fact that when dealing with var optimization, most optimization procedures described in the literature focus upon reactive power rescheduling and not reactive reserve margin optimization. In the realm of mid-term voltage stability, the reactive reserve margin is extremely important at generators because it gives an advance indication of how close the generator might be to its OEL becoming active. Conceivably, a weak area could become weaker if a generator's OEL would operate in a stressed situation because of the simple reason that its reactive capability would be exhausted. In turn, this would lead to the area importing reactive power from neighboring areas, thus creating an onerous situation for a collapse to occur.

Appendix

This Appendix shows the reduced WECC System, which is shown in Fig. 6.

References

[1] A. M. Abed, "WSCC voltage stability criteria, under-voltage, load shedding strategy, and reactive power reserve monitoring methodology," in *Proc. IEEE Power Engineering Society Summer Meeting*, vol. 1, Edmonton, AB, Canada, Jul. 1999, pp. 191–197.

[2] Z. Feng, W. Xu, C. Oakley, and S. Mcgoldrich, "Experiences on assessing alberta power system voltage stability with respect to the WSCC reactive power criteria," in *IEEE Power Engineering Society Summer Meeting*, vol. 2, Edmonton, AB, Canada, Jul. 1999, pp. 1297–1302.

[3] B. H. Chowdhury and C. W. Taylor, "Voltage stability analysis: V-Q power flow simulation versus dynamic simulation," *IEEE Trans. Power Syst.*, vol. 15, no. 4, pp. 1354–1359, Nov. 2000.

[4] P. Nedwick, A. F. Mistr Jr., and E. B. Croasdale, "Reactive management a key to survival in the 1990s," *IEEE Trans. Power Syst.*, vol. 10, no. 2, pp. 1036–1043, May 1995.

[5] R. A. Schlueter, "A voltage stability security assessment method," *IEEE Trans. Power Syst.*, vol. 13, no. 4, pp. 1423–1438, Nov. 1998.

[6] E. Vaahedi, Y. Mansour, C. Fuchs, S. Granville, M. D. L. Latore, and H. Hamadanizadeh, "Dynamic security constrained optimal power flow/var planning," *IEEE Trans. on Power Systems*, vol. 16, no. 1, pp. 38–43, Feb. 2001.

[7] T. Menezes, L. C. da Silva, and V. F. da Costa, "Dynamic VAR sources scheduling for improving voltage stability margin," *IEEE Trans. Power Syst.*, vol. 18, no. 2, pp. 969–971, May 2003.

[8] E. Vaahedi, J. Tamby, Y. Mansour, L. Wenyuan, and D. Sun, "Large scale voltage stability constrained optimal VAr planning and voltage stability applications using existing OPF/optimal VAr planning tools," *IEEE Trans. Power Syst.*, vol. 14, no. 1, pp. 65–74, Feb. 1999.

[9] C. W. Taylor and R. Ramanathan, "BPA reactive power monitoring and control following the august 10, 1996 power failure," in *Proc. VI Symp. Specialists in Electric Operational and Expansion Planning*, Salvador, Brazil, May 1998.

[10] C. W. Taylor, *Power System Voltage Stability*. New York: McGraw-Hill, 1994.

[11] S. B. Mokhtar, H. D. Sherali, and C. M. Shetty, *Nonlinear Programming Theory and Algorithms*, 2nd ed. New York: Wiley, 1993.

[12] T. Gomez, J. Lumbreras, and V. M. Parra, "A security-constrained decomposition approach to optimal reactive power planning," *IEEE Trans. Power Syst.*, vol. 6, no. 3, pp. 1069–1076, Aug. 1991.

[13] S. Granville, M. Candida, and A. Lima, "Application of decompostion techniques to var planning: Methodological & computational aspects," *IEEE Trans. Power Syst.*, vol. 9, no. 4, pp. 1780–1787, Dec. 1994.

[14] G. Astfalk, I. Lustig, R. Marstern, and D. Shanno, "The interior point method for linear programming," *IEEE Software*, vol. 9, no. 4, pp. 61–68, Jul. 1992.

[15] S. Granville, "Optimal reactive dispatch through interior point methods," *IEEE Trans. Power Syst.*, vol. 9, no. 1, pp. 136–146, Feb. 1994.

[16] *EUROSTAG Package Documentation*, May 1999. Tractebel Energy Engineering, Release 3.2.

Feng Dong (S'03) received the B.S. and M.S. degrees in electrical engineering from Hohai University, Nanjing, China, in 1995 and 1999, respectively. He is currently pursuing the Ph.D. degree in the Department of Electrical and Computer Engineering, University of Missouri-Rolla.

Badrul H. Chowdhury (S'86–M'87–SM'92) received the M.S. and Ph.D. degrees in electrical engineering from Virginia Tech, Blacksburg, VA, in 1983 and 1987, respectively.

He is currently a Professor in the Electrical and Computer Engineering Department, University of Missouri-Rolla.

Mariesa L. Crow (S'83–M'90–SM'94) received the B.S.E.E. degree from the University of Michigan, Ann Arbor, and the Ph.D. degree from the University of Illinois at Urbana–Champaign in 1989, both in electrical engineering.

She is currently Associate Dean for Graduate Studies and Research and a Professor of Electrical and Computer Engineering at the University of Missouri-Rolla.

Levent Acar (M'86–SM'88) received the M.S. and Ph.D. degrees in electrical engineering from The Ohio State University, Columbus, OH, in 1984 and 1988, respectively.

He is currently an Associate Professor in the Electrical and Computer Engineering Department, University of Missouri-Rolla.